

Advanced Journal of Environmental Science and Technology ISSN 2756-3251, Vol. 16 (11), pp. 001-006, November, 2025. Available online at www.internationalscholarsjournals.org © International Scholars Journals

Author(s) retain the copyright of this article.

Full Length Research Paper

Comparative study of the thermal behavior of the modeled kiln and the experimental kiln used for ceramics firing in northern Togo

*KATA. N'Detigma¹, KPODE Kodjo¹, SAMAH Hodo-Abalo¹

¹LaMERE, Laboratoire Matériaux, Energie Renouvelable et Environnement; Kara University, Kara, Togo.

Abstract

Received 21 September, 2025; Revised 02 November, 2025; Accepted 06 November, 2025; Published 16, 2025

This study consisted of validating a furnace model through a comparative analysis of simulation and experimental data. The gas kiln converted into a wood kiln was modeled using Comsol Multiphysics software and simulated based on Navier-Stokes equations. A metric study was conducted, as well as graphical representations, to evaluate the consistency between the simulation results and those of experimental measurements. The value of the bias measures the accuracy of a model and indicates the extent to which an estimation method tends to overestimate or underestimate reality. On the other hand, the confidence interval (CI) that we use helps to assess the reliability of the model's results. Based on the visual observation of the temperature profile over time, the simulated values seem to match the experimental ones. The comparative analysis of the experimental and simulated temperature profiles gives a bias value of -5.58 and a 95% confidence interval (CI) containing zero (0), which shows that there's no significant systemic bias. The RMSE value (33.63) and MAPE value (~7.35%) show an acceptable average error between the experiment and the simulation. A high R² value indicates a satisfactory correlation between the simulation and the experiment.

Keywords: Carbon footprint, Ceramics, Thermal, Simulation, Togo.

1. Introduction

One of the most energy-intensive stages in the ceramic manufacturing process is firing. It can require up to 50% of the total energy consumption in a workshop or factory [1]. At this stage, temperatures can vary from 800°C to 1400°C depending on the type of kiln. As a result, there is a high demand for energy, which inevitably has a significant carbon footprint [2]. According to the International Energy Agency (IEA), 10% of global industrial energy consumption is generated by the materials sector, a substantial proportion of which is

attributable to thermal firing processes [3]. Research into energy management during ceramic firing will not only reduce costs, but also enhance environmental sustainability.

Boudrahem et al. mentioned energy optimization and environmental assessment in ceramic production in their study. Several studies have examined improvement scenarios based on life cycle and technical-economic analyses [4].

Zhou et al. proposed integrating renewable energies into ceramic kiln systems to reduce their carbon footprints [5]. The kilns used in sub-Saharan Africa in large part and in Togo in particular are open kilns and subject to heavy energy loss.

In the Pouwédéou women's community in Pya Pittah, Kara, northern Togo, a gas kiln was donated to the community to reduce their exposure to smoke and high external temperatures from the previous kiln. Beyond the fact that gas kilns pose a carbon footprint concern, access to this fuel was limited

To overcome gas supply difficulties, the kiln was converted to wood-fired without any particular modifications. The result is that the modification is still not satisfactory for users because it raises an issue of identity for the finished ceramic product, to which users are attached. The firing temperature of this modified kiln no longer allows certain identifying marks to be preserved on the ceramics produced. This raises the question of what improvements could be made to the kiln to ensure its local acceptance by African societies attached to traditional historical and cultural values. The study of such parameters requires modeling the kiln, validating the current parameters of the model, and analyzing its thermal behavior in order to propose, through simulation, a temperature profile that takes into account the identity of the ceramic product.

This study, entitled "Comparative study of the thermal behavior of the modeled kiln and the experimental kiln used for firing ceramics in northern Togo," fits into this context. The objective of the approach is to justify the scientific relevance of the numerical data that we will use for proposals to modify the kiln.

2. Materials and Methodology

2.1. Numerical modeling software.

For modeling, Comsol Multiphysics software is used. This software is widely used in several research projects for a variety of model and physics simulations [6] [7] [8]. It offers a powerful integrated environment with a model generator and access to the required features. From coupling physical phenomena to automatically creating sequences, COMSOL Multiphysics offers features for geometric design, meshing, studies. resolution parameters, and result previews. The software is suitable for modeling in several fields (mechanics, thermodynamics, electromagnetism, etc.). Depending on the topic being addressed, Comsol can couple the differential equations of several physical phenomena.

This study involves mechanics, fluid flow, and thermics. The classical heat equation in this case is given as follows:

$$\rho C_p \frac{\partial T}{\partial t} + \rho C_p U \nabla T = \nabla \cdot (k \nabla T) + Q \tag{1}$$

Où T(x,t): temperature; ρ : density;

 C_p : heat capacity;

k: thermal conductivity;

Q: heat source;

U: velocity field (convection case).

The equations that model the phenomena involved are solved using the finite element method. This method is the standard for calculating solutions to elliptic, parabolic, and hyperbolic boundary value problems [9]. The boundary integration conditions are imposed as follows: When the condition is an equation imposed on a given surface, Dirichlet boundaries are applied:

$$T = T_0 \tag{2}$$

In the case of a heat flux being applied, the Neumann condition is applied

$$-k\nabla T.\,n = q_0\tag{3}$$

Where n denotes the unit normal vector to the boundary surface Γ

For convective exchanges, Robin's condition is applied:

$$-k\nabla T. n = h(T - T_{\infty}) \tag{4}$$

Discretization is performed using finite elements derived from the domain mesh. Temperature T is approximated by a combination of local shape functions N_i

The discretization equation is given by:

$$T(x,t) \approx \sum_{i} N_i(x) T_i(t)$$
 (5)

In Comsol, equation (1) is automatically constructed in the form of equation (6) when the operator adds the "Heat transfer" module.

$$\int_{\Omega} \rho C_{p} \frac{\partial T}{\partial t} \nu \, d\Omega + \int_{\Omega} \rho C_{p} (U \nabla T) \nu \, d\Omega + \int_{\Omega} k \nabla T \cdot \nabla \nu \, d\Omega$$

$$= \int_{\Omega} Q \nu \, d\Omega + \int_{\Gamma_{q}} q_{0} \nu \, d\Gamma \tag{6}$$

With

 ν : test function;

 Ω : integration domain;

 q_0 : imposed heat flux;

 Γ : border at the edge of the domain Ω ;

This equation is taken into account by Comsol in the following form where ν is defined by N_i :

$$[M]\frac{dT}{dt} + [K]T = F \tag{7}$$

Where

[M] is a mass matrix $\int_{\Omega} \rho C_p N_i N_j d\Omega$

[K] is the thermal stiffness matrix $\int_{\Omega} k \nabla N_i . \nabla N_j \ d\Omega$

F a load vector defined by $\int_{\Omega} QN_iN_j d\Omega$

The time steps and mesh are adjusted to achieve the accuracy desired by the operator. ComSol uses numerical time and linear solvers.

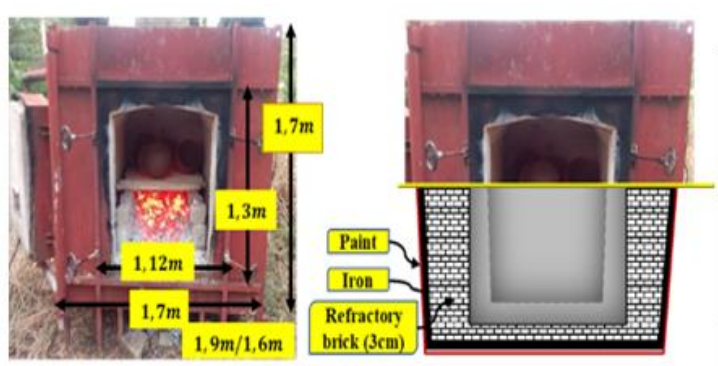


Figure 1: Technical characteristics of the kiln.

layer of anti-rust paint (figure 1). It has two inlets and a chimney: an air inlet at the bottom of the kiln consisting of eight (8) isosceles triangular holes measuring 11/10 cm on each side, also used for ash removal; an air inlet at the front of the kiln measuring 0.2 m high, 0.3 m wide, and 0.23 m deep; a chimney with the same dimensions as the front air inlet.

On the dome, smoke escapes through six holes measuring 0.07 m on each side [10].

Experimental tests were carried out with four (04) pieces measuring 25 cm in diameter and 35 cm in height, which were fired for 2 hours and 10 minutes. The temperature parameter was measured in order to facilitate the validation of the modeling results.

The ComSol model of this kiln was created taking into account all the parameters of the FMB kiln. The table 1 provides data on the thermal properties of the materials integrated into ComSol for the simulation.

2.3. Method of analyzing results

The error measurement made relating to the reliability and quality of the values of the simulated furnace model. Thus, considering y_i the experimental value and \hat{y}_i the simulated value and N the number of observations.

The mean error (bias) is calculated by:

$$\frac{1}{N} \sum_{i=1}^{N} (\hat{y}_i - y_i)$$
 (8)

The Mean Absolute Error (MAE) is obtained by:

$$MAE = \frac{1}{N} \sum_{i=1}^{N} |\hat{y}_i - y_i|$$
 (9)

RMSE (Root Mean Square Error) is calculated by:

The software has an extensive material library and can be customized.

2.2. The Modern Wood-Fired Kiln (FMB).

The FMB kiln on which we are conducting this digital study consists of three (3) layers. A layer of heat-resistant bricks 3 cm thick; a layer of ferrous metal and a

Table 1: Properties of materials used for simulation

	Materials	Density (kg/m³)	Heat capacity at constant pressure (J/Kg.K)	Thermal conductivity (W/m.K)	
	Heat resistant brick	2500	732	0.5	
	Polished iron	56	449	80	

$$\sqrt{\frac{1}{N} \sum_{i=1}^{N} (\hat{y}_i - y_i)^2}$$
 (10)

MAPE (Mean Absolute Percentage Error) is determined by;

$$MAPE = \frac{100\%}{N} \sum_{i=1}^{N} \left| \frac{\hat{y}_i - y_i}{y_i} \right|$$
 (11)

The coefficient of determination is obtained by:

$$R^{2} = 1 - \frac{\sum_{i=1}^{N} (\hat{y}_{i} - y_{i})^{2}}{\sum_{i=1}^{N} (y_{i} - \bar{y})^{2}}$$
(12)

Where \bar{y} is the mean of the measured values Bland-Altman and parity graphs are used to verify the concordance of the measured and simulated values. These graphs also allow us to verify whether the simulation model is equivalent and interchangeable with the actual kiln and could be used for future testing.

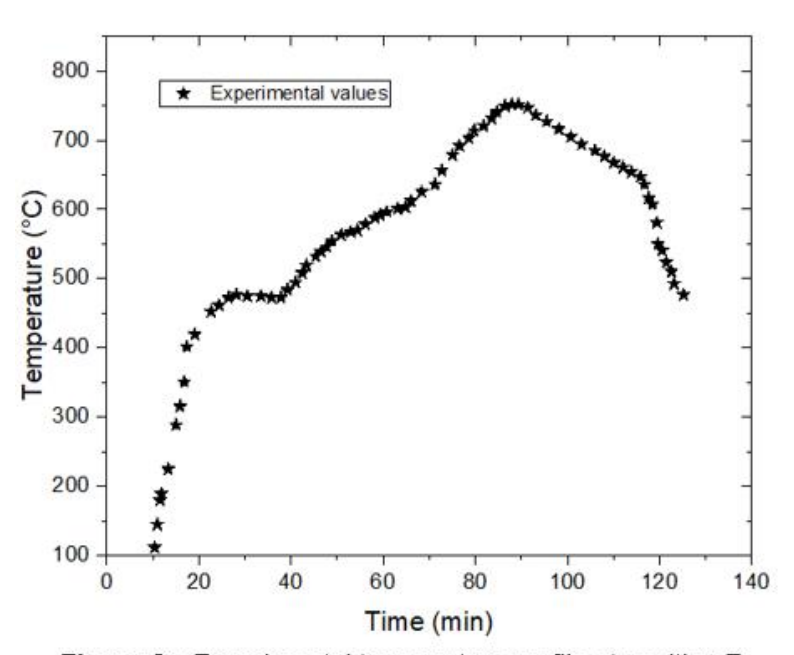
3. Results and discussions.

3.1 Experimental results

Temperature sensors placed inside the kiln were used to record the kiln's temperature profile

Two firing phases are easily identifiable in this profile (figure 2): the temperature rise and the cooling phase.

The temperature rise phase: this is not regular. It is erratic because the inside of the kiln is exposed to gusts



0.5

Figure 2: Experimental temperature profile at position Z

Figure 3: Hot air rising in the kiln.

of wind when the kiln is opened to check the appearance of the ceramics being fired. Traditionally, potters do not have sensors to monitor the temperature of the kiln. She opens the kiln from time to time and visually inspects the color of the source. When the source turns bright red, the kiln operator considers the temperature to be satisfactory. The drop in temperature observed after 30 minutes of firing reflects the moment when the kiln operator decided it was necessary to add wood in order to continue the temperature rise.

The cooling phase: In this experiment, this occurs approximately 80 minutes after the furnace has stopped being fed with wood. This time varies and depends on the amount of biomass fuel introduced into the furnace and the number of ceramics to be fired.

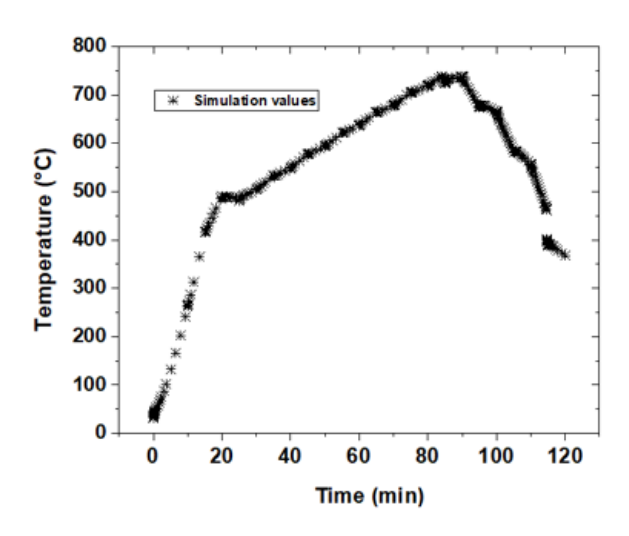


Figure 4: Numerical simulation at point z

3.2 Simulation results.

The simulation took into account the actual conditions during the experiment. This involved introducing four (04) pieces measuring 25 cm in diameter and 35 cm in height. Although the position of the ceramics did not obstruct the flow of hot air coming directly from the heat source, it changed its flow, which is no longer laminar, as can be seen in the figure 3. When the air is heated by the source, a temperature gradient is established, causing the hot air to move from the bottom to the top, as illustrated in Figure 3 of the simulation.

Thermal transfer phenomena within the kiln are studied by monitoring changes in the average air temperature at point z inside the kiln: T(z,t) [6].

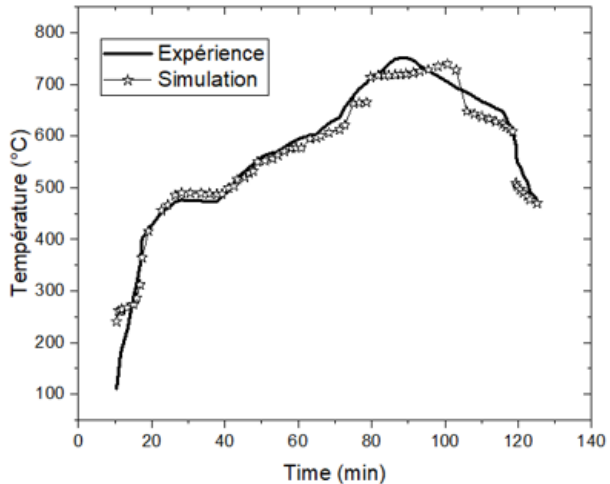


Figure 5 Temporal evolution of the temperature of the experimental and simulated kiln

The use of heat-resistant bricks minimizes heat loss through the kiln walls.

Navier-Stokes equations are solved using the following conditions:

Initial conditions:

$$u(x;0) = \frac{0.2m}{s}$$
 $T(x;0) = 305,15K$ (13)

Limit conditions:

$$k \frac{\partial T}{\partial t} \Big|_{I} = h \frac{\partial T}{\partial t} \Big|_{I} \tag{14}$$

The figure 4 shows the temperature profile inside the kiln. The disturbances observed when opening the kiln to check combustion or add fuel are less significant.

Overall, the temperature profile appears to correspond to that obtained experimentally. In addition, a metric study and Bland-Altman and parity representations are used to analyze the correspondence between the two types of values.

3.3 Comparative Study of Results.

The table 2 summarizes the error measurements performed on the experimental values and simulation values.

The bias value of -5.58 would suggest a slight underestimation of the temperature profile by the simulation. However, the 95% CI value containing zero (0) indicates a good absence of significant systemic bias.

Table 2: summarizes the error measurements.

N	Average bias	IC 95%	MAE	RMSE	MAPE	\mathbb{R}^2
71	-5.58	[-12.94, 2.36]	23.7	33.63	≈ 7.35	0.96

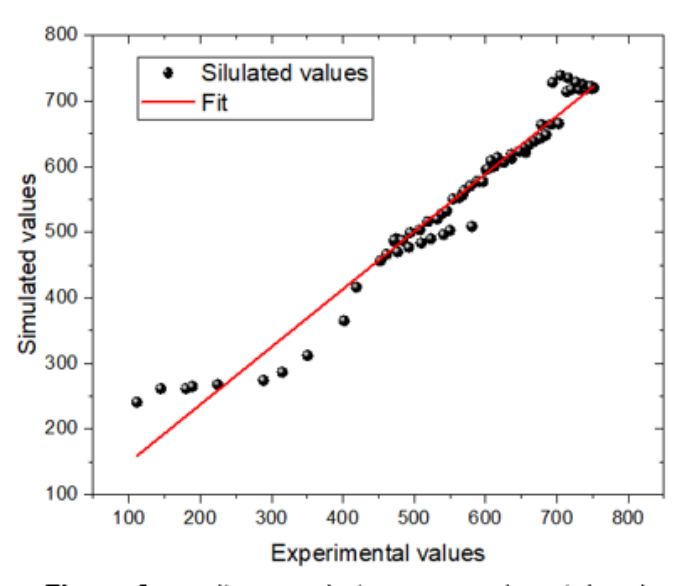


Figure 6 : parity curve between experimental and simulated temperature

The RMSE value (33.63) and the MAPE value (~7.35%) show an acceptable average error between the experiment and the simulation. The R² value (0.96) is high and indicates a satisfying correlation between the simulation and the experiment.

The following graphs (figure 5) show the agreement and any zones of divergence between the simulated values and the experimental values.

Observation of the results in the figure shows good visual agreement with a few isolated discrepancies. However, analysis of the parity curve (figure 6) shows that even though most of the points follow the equation y=x, there are some significant deviations. This significant

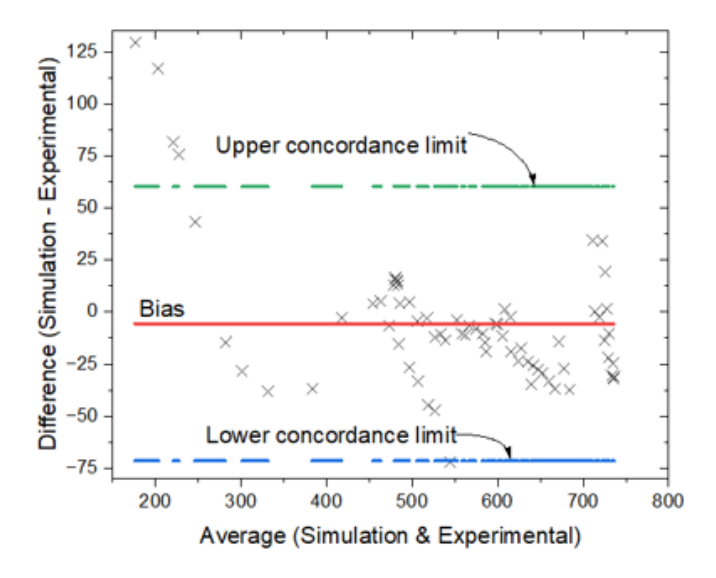


Figure 7: The Bland-Altman concordance diagram

dispersion between the experimental values and the simulation for certain points (especially at low temperatures) is illustrated by the Bland-Altman plot (figure 7) with a wide range of agreement limits of ± 70 . These results demonstrate the accuracy of the kiln model and can be used for studies enabling the preservation of the identity marks of ceramics fired in this type of kiln.

Conclusion

The mathematical model established through this study of the operation of a pottery kiln in northern Togo has shown how the kiln's ambient temperature changes over time. There is a combined heat exchange system that results in a kind of energy saving. The experimental and numerical temperature profiles show a similarity that lends credence to the kiln model developed with Comsol Multiphysics software, which we will adopt in our continued work on this kiln converted into a wood-fired kiln. Comparative analysis of the experimental and simulated temperature profiles gives a bias value of -5.58 and a 95% CI containing zero (0), indicating a good absence of significant systemic bias.

The RMSE value (33.63) and the MAPE value (~7.35%) show an acceptable average error between the experiment and the simulation. A high R² value shows a satisfying correlation between the simulation and the experiment.

The results of this study lay the foundations for a digital study of kilns with a view to preserving the African identity marks left on Togolese ceramics.

REFERENCES

- [1] Fang, X., Li, J., & Wang, Z. (2021). Thermal energy analysis and waste heat recovery in ceramic kilns. Applied Thermal Engineering, pp. 188, 116643.
- [2] Kumar, S., Singh, R., & Tiwari, A (2020) Energy consumption and efficiency improvement in ceramic manufacturing industries: A review. Journal of Cleaner Production, pp. 277, 123420.
- [3] AIE (Agence Internationale de l'Énergie), «Energy Efficiency 2022 Report,» Paris: International Energy Agency., 2022.
- [4] Boudrahem, F., Drouiche, N., & Lounici, H., «Energy optimization and environmental

- assessment in ceramic production.,» *Environmental Technology*, vol. 40, n° %110, p. 1264–1273, 2019.
- [5] Zhou, Y., Wu, H., & Li, Q (2023). Renewable energy integration in ceramic kiln systems for carbon footprint reduction. Renewable Energy, vol. 205, p. 87–98.
- [6] Carasi, Beatrice (2017). SIMULATING HEAT TRANSFER PHENOMENA WITH COMSOL MULTIPHYSICS. Proceedings of CHT-17 ICHMT International Symposium on Advances in Computational Heat Transfer. pp. https://doi.org/10.1615/ichmt.2017.cht-7.620.
- [7] Vajdi, M., Moghanlou, F., Sharifianjazi, F., Asl, M., & Shokouhimehr, M. (2020). A review on the Comsol Multiphysics studies of heat transfer in advanced ceramics. Journal of Composites and Compounds. https://doi.org/10.29252/jcc.2.1.5.
- [8] Kadyrmjatov, Y., Safin, A., Petrov, T., & Basenko, V. (2025) Application of COMSOL Multiphysics for Modeling Wireless Charging Systems. 2025 7th International Youth Conference on Radio Electronics, Electrical and Power Engineering (REEPE), pp. 1-5.
- [9] G. ALLAIRE (2007). Analyse numérique et Optimisation,, Paris: Ecole Plytechnique.
- [10] KATA N'DEtigma, Sizing E, SAMAH Hodo-Abalo (2025). Experimental study of the thermal behavior of the traditional open-air oven in Northern Togo. 5th International Conference on Innovative Research in Applied Science, Engineering and Technology (IRASET).